

University of Groningen

Organic field-effect transistors for sensing applications

Maddalena, Francesco

IMPORTANT NOTE: You are advised to consult the publisher's version (publisher's PDF) if you wish to cite from it. Please check the document version below.

Document Version

Publisher's PDF, also known as Version of record

Publication date:

2011

[Link to publication in University of Groningen/UMCG research database](#)

Citation for published version (APA):

Maddalena, F. (2011). *Organic field-effect transistors for sensing applications*. [Thesis fully internal (DIV), University of Groningen]. [s.n.].

Copyright

Other than for strictly personal use, it is not permitted to download or to forward/distribute the text or part of it without the consent of the author(s) and/or copyright holder(s), unless the work is under an open content license (like Creative Commons).

The publication may also be distributed here under the terms of Article 25fa of the Dutch Copyright Act, indicated by the "Taverne" license. More information can be found on the University of Groningen website: <https://www.rug.nl/library/open-access/self-archiving-pure/taverne-amendment>.

Take-down policy

If you believe that this document breaches copyright please contact us providing details, and we will remove access to the work immediately and investigate your claim.

Downloaded from the University of Groningen/UMCG research database (Pure): <http://www.rug.nl/research/portal>. For technical reasons the number of authors shown on this cover page is limited to 10 maximum.

Chapter 6

Carrier Density Dependence of the Hole Mobility in Doped and Undoped Organic Semiconductors

Abstract

The charge carrier mobility in conjugated polymers depends on the charge carrier density. Here we investigate the mobility of poly(3-hexylthiophene) over a carrier densities range from 10^{15} cm^{-3} to 10^{20} cm^{-3} in order to experimentally establish the relation between mobility and carrier density. Hole-only diodes were used for low densities and field-effect transistors were used for the high carrier densities. Intermediate densities were probed using chemically doped Schottky diodes and transistors. We demonstrate that the mobility is constant for carrier densities below 10^{16} cm^{-3} and follows a power law dependence for carrier densities higher than 10^{18} cm^{-3} . We also make note of possible anomalies rising from trapping effects or morphology.

* Part of this work was published as J. J. Brondijk, F. Maddalena, K. Asadi, H. J. van Leijen, M. Heeney, P. W. M. Blom and D. M. de Leeuw, Physica Status Solidi B, accepted (2011).

6.1 Introduction

Solution-processable conjugated polymers such as polythiophene derivatives are attractive candidates for application in low-cost and flexible microelectronic devices. The electrical transport in semiconducting polymers is dominated by thermally assisted intermolecular hopping of the charge carriers in a Gaussian density of states [1]. The transport depends on carrier density, temperature and electric field [2, 3, 4, 5, 6]. At room temperature and at relatively small electric field the transport is dominated by the carrier-density and the field dependence plays a negligible role [6, 7]. Experimentally capturing the full extent of the relation between mobility and carrier density is necessary for understanding and improvement of device performance. For poly(p-phenylene vinylene) derivatives, the mobility extracted from diodes is relatively low, around 10^{-7} cm²/Vs, and independent of carrier density. The mobility extracted from field-effect transistors however increases with charge carrier density up to typically 10^{-3} cm²/Vs. The difference originates from the charge carrier density, which in diodes is typically 10^{15} cm⁻³ to 10^{16} cm⁻³ and in transistors from 10^{18} cm⁻³ to 10^{20} cm⁻³ [8]. However, a full mobility carrier-density relation is hindered by a gap in the carrier density between 10^{16} cm⁻³ to 10^{18} cm⁻³ [8, 9].

Polythiophenes have been extensively applied in organic field-effect transistors (OFETs) [10, 11] and solar cells [12]. Recently polythiophene and its derivatives have found applications in the field of chemical sensors and biosensors [13, 14]. The benchmark polythiophene is regioregular poly(3-hexyl-thiophene) (rr-P3HT). Doping in organic semiconductors has been an important topic since the introduction of these semiconductors [15, 16]. More recently achievements have been made in the field of stable n-type doping and solution-processed doping [17, 18, 19].

To probe the charge carrier mobility in the region between 10^{16} cm⁻³ to 10^{18} cm⁻³, we deliberately doped rr-P3HT [20]. In this work we investigated hole-only diodes, (doped) Schottky diodes and (doped) transistors. In this way over the whole range of charge carrier densities, the mobility can be unified by a zero-field mobility with a density dependent term based on hopping in an exponential density of states (DOS) [8, 21].

6.2 Results and discussion

To chemically dope rr-P3HT (the polymer was obtained from M. Heeney, Imperial College London), we exposed the devices to vaporized trichloro-(1*H*, 1*H*, 2*H*, 2*H*)-perfluorooctylsilane (TCFOS; Sigma Aldrich) at a partial pressure of $\sim 2.5 \cdot 10^{-1}$ mbar (see *chapter 2, section 2.3.3*). The transfer characteristics of the transistors were measured as a function of exposure time [22]. We note that in the case of Schottky diodes the evaporation of the top electrode was performed after the doping process to guarantee a uniformly doped semiconductor layer.

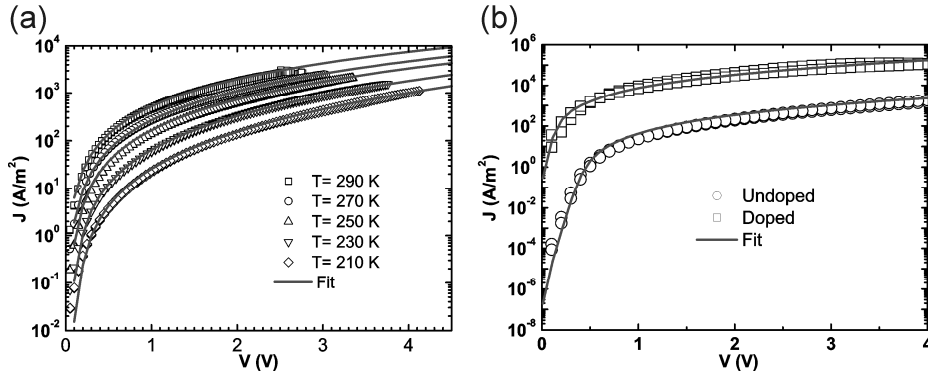


Figure 1. (a) Current density versus voltage for a rr-P3HT hole-only diode with a thickness of 135 nm measured as a function of temperature. The solid lines represent the fit according to the carrier density-dependent and field-dependent mobility model. (b) Current density versus voltage of an undoped and a doped Schottky diode with a thickness of 195 nm. The solid lines represent the fit according to the model.

The current density of a rr-P3HT hole-only diode as a function of applied voltage is presented in Figure 1 a. The transport was measured as a function of temperature. At low bias the current density scales at low bias with the voltage squared, indicating space-charge-limited current (SCLC) with a constant mobility. The injecting contact was PEDOT:PSS, which is an Ohmic contact to rr-P3HT, because the work function matches the energy of the highest occupied molecular orbital (HOMO) of rr-P3HT [23]. The transport in the diode is then bulk limited. At high bias the current density is enhanced. Charge transport is due to thermally activated hopping between localized states at the Fermi level. Device simulations were performed by using a numerical drift-diffusion model [24], incorporating a hopping mobility that depends on both charge-carrier density and electric field [21,

25, 26]. Figure 1 a shows that for all temperatures a perfect agreement between measured and calculated current densities is obtained. As fit parameters we used a room temperature zero-field mobility of $1.5 \times 10^{-4} \text{ cm}^2 \text{ V}^{-1} \text{ s}^{-1}$ with an activation energy of about 0.2 eV, a zero-field conductivity of $5 \times 10^6 \text{ Sm}^{-1}$ a characteristic temperature for the exponential DOS, T_0 , of 475 K and overlap parameter α^{-1} of 3 Å. The numbers agree well with reported values for rr-P3HT [Error! Bookmark not defined.]. We note that at room temperature and for the low applied bias the density dependence dominates and the electric field dependence is negligible. To extract from the fit the charge carrier density mobility relation we used the procedure reported by Craciun *et al.* [9]. The mobility is presented later (page 80) as a function of average charge density in Figure 4.

In order to increase the charge carrier density in diodes we fabricated doped Schottky diodes. As a reference, however, first undoped diodes were investigated. The Schottky diodes exhibit a rectification of more than 6 orders of magnitude. The current in forward bias is presented in Figure 1 b. The current density is calculated with the same numerical model as for the hole-only diodes using identical fit parameters. The solid line in Figure 1 b shows that a good agreement between calculated and measured current densities is obtained. To increase the carrier density Schottky diodes were doped. Exposing rr-P3HT to vaporized TCFOs yields *p*-type doping with additional mobile holes [20, 22]. Figure 1 b shows that the current density in forward bias increases. The origin is an increase in mobility due to an increased charge density. To quantify the relation we determined the charge carrier density independently from CV measurements in reverse bias.

In order to determine the acceptor density of the dopant in the semiconductor we used impedance spectrometry. An AC voltage of 100 mV was superimposed to the applied reverse DC bias. A frequency scan from 10 Hz to 1 MHz was made at each bias and the equivalent parallel capacitance (C_p) was extracted. Figure 2 shows C_p^{-2} versus reverse V_{DC} for a diode exposed 20 minutes to TCFOs vapor. A straight line is obtained. The acceptor density, N_A , was calculated with the Mott-Schottky relation, from the slope of the variation of the C_p^{-2} with DC bias V_{DC} :

$$N_A = \frac{2}{q\epsilon_0\epsilon_s} \left(-\frac{1}{\partial(1/C_p^2)/\partial V_{DC}} \right) \quad (6.1)$$

where q is the elementary charge, ϵ_0 is the dielectric constant in vacuum and ϵ_s is the relative dielectric constant of the semiconductor.

The extracted value was then used as an input to calculate the forward current density. The solid line in Figure 1 b shows that a good agreement is obtained. From

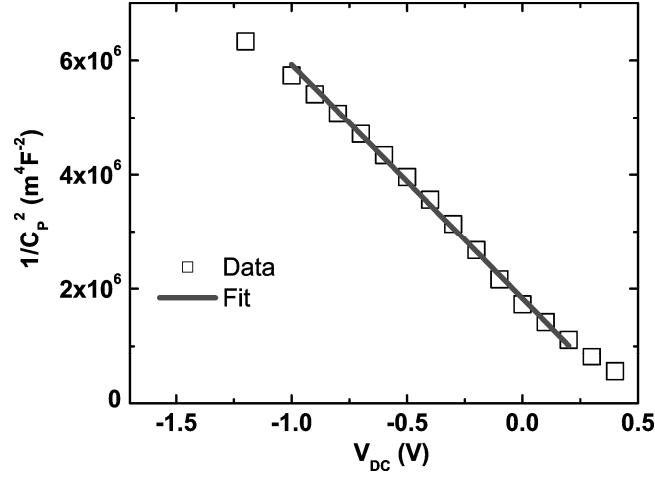


Figure 2. Inverse of the capacitance squared versus DC bias of the doped Schottky diode from Figure 1 b. The solid line represents the linear fit.

the calculation, the corresponding average mobility was extracted. For three doped Schottky diodes the mobility is presented as a function of charge carrier density in Figure 4 in the next page.

To probe the mobility at high carrier density field-effect transistors were investigated. The carrier density quadratically decreases with the distance from the semiconductor gate-dielectric interface. The density at the interface dominates the transport and was calculated as reported previously [27]. The field-effect mobility μ_{FE} was approximated at each gate bias using the relation [28]:

$$\mu_{FE} = \frac{L}{WC_I V_d} \frac{\partial I_d}{\partial V_g} \quad (6.2)$$

where L and W are the length and width of the channels of the OFET respectively, C_I is the capacitance per unit area of the gate insulator, V_d is the drain current and V_g is the gate bias. The extracted mobility versus carrier density values for an undoped rr-P3HT transistor are presented in Figure 4.

Exposing the transistors to TCFOS vapor leads to doping of rr-P3HT. The doping density can be varied by changing the exposure time. Transfer curves were recorded in-situ at different exposure times are presented in Figure 3. A shoulder appears in the transfer curve; a higher positive bias is needed to deplete the doped bulk semiconductor and pinch-off the channel. Also the on-current at negative gate

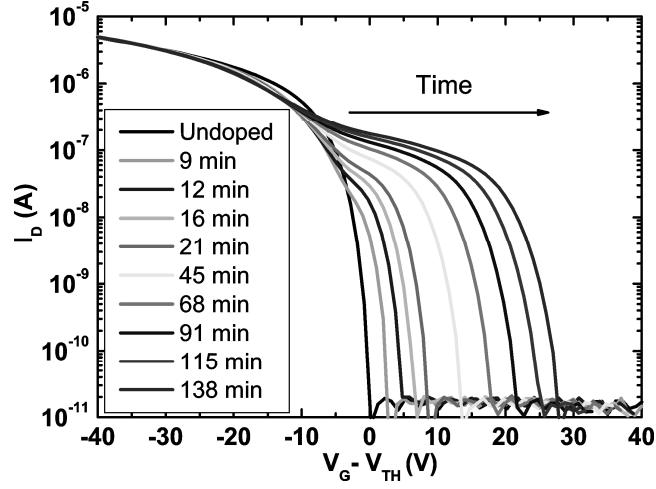


Figure 3. Transfer curves in the linear regime of a rr-P3HT organic field-effect transistor in vacuum before and after exposure to TCFOS vapor at room temperature for different exposure times. The channel length and width are 10 μm and 2500 μm respectively. The transfer curves are corrected for the switch-on voltage shift with respect to the pristine undoped transistor at $t=0$. [8] The threshold voltages range from 5.8 V for the undoped transistor to 19 V after 138 min.

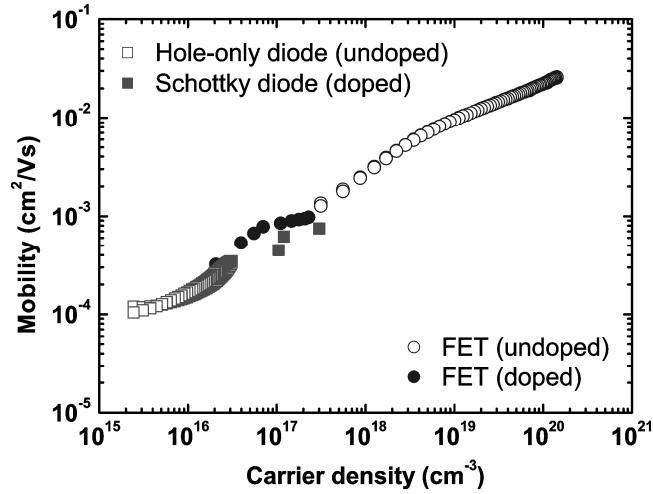


Figure 4. Charge carrier mobility versus carrier density as derived for rr-P3HT from undoped hole-only diodes, doped Schottky diodes, and undoped and doped field-effect transistors.

CHAPTER 6

bias, in accumulation, slightly increases due to a shift in threshold voltage. The threshold voltage, defined as the onset of the channel current at flatband [29], shifts to positive values upon doping. Each transfer curve in Figure 3 is corrected for its threshold voltage indicating that the accumulation currents are identical within experimental error. The corrected transfer curves show a cross-over from an accumulation mode into a bulk depletion mode transistor [22, 30]. The current in accumulation is dominated by the channel current, while in depletion, at positive gate bias, the current is mainly flowing through the bulk semiconductor. The doping density can be calculated from the pinch-off voltage [22, 30] and the mobility can be calculated from the current at flat band conditions at zero gate bias normalized for the shift in threshold voltage [22, 30]. The extracted mobilities and carrier densities are presented in Figure 4 as well.

The extracted mobility and charge carrier density values from all devices investigated are presented in Figure 4. The gap between the undoped diodes and undoped transistors is probed with the doped diodes and the doped transistors. Moreover Figure 4 shows that the hole mobility is flattening for charge carrier densities below 10^{16} cm^{-3} and increases with a power law for higher charge densities. The power law dependence is due to hopping transport in disordered semiconductors [8, 21]. Slight deviations from the power law at intermediate density might be due to anisotropy in the charge transport caused by the nanocrystalline nature of rr-P3HT.

6.3 Anomalous behavior

In some cases, however, we find that the dependence of mobility on charge density deviates from the power law trend expected from the Vissenberg and Matters and Tanase et al. (VMT) transport model [8, 21]. Figure 5 shows the charge carrier mobility versus carrier density derived from undoped hole-only diodes, undoped and doped field-effect transistors for rr-P3HT (Rieke Chemicals) and poly(2-methoxy-5-(2'-ethylhexyloxy)-1,4-phenylene vinylene) (MEH-PPV, Merck). MEH-PPV, shows that the trend according to the VMT model of charge carrier mobility versus charge density observed above still holds for other materials other than the polythiophene studied above. On the other hand the data from rr-P3HT (Rieke) shows a clear anomaly from the trend expected from the VMT model. Although the mobility versus charge carrier density relationship between

the two different batches of rr-P3HT are quite similar for undoped diodes and OFETs, there is a clear difference in the relationship obtained from doped OFETs in the gap between low and high charge carrier densities. The mobility increases sharply, with a power law relationship higher than the one expected from the VMT model. Such anomaly has been observed before for other batches of rr-P3HT and for poly(2,5-thienylene vinylene) (PTV) [30].

The reason for such anomaly can be threefold. First the anomaly could rise from a difference in morphology. Different batches of rr-P3HT, might have been synthesized in different conditions or by different synthetic route. Moreover, even if the synthetic process for two different batches of semiconducting polymers is kept constant, some small differences in the end products might still arise. Such differences might cause a change in the overall regioregularity and average chain length of the polymers, hence in the overall morphology of spin-coated films [31]. Moreover, in a solid thin film of a single material there may be a significant difference in morphology of the polymer between the semiconductor/insulator interface region where field-effect conduction in OFETs occurs and the bulk of the material, where bulk conduction occurs in diodes and doped OFETs. Since the hopping rate of charge carriers, which determines the mobility and conduction in semiconducting polymers, strongly depends on the morphology [32], the differences in the morphology will strongly influence conduction. Hence the sharp increase in mobility with charge carrier density due to chemical doping, might be the result of different morphologies between different materials or within the spincoated thin films, as it was previously explained for similar behavior in rr-P3HT and PTV [30, 33]. Therefore, the study of the interface and bulk morphology of disordered organic semiconductors is of great importance in OFETs, especially if the bulk conduction becomes relevant such as in the case of doped transistors.

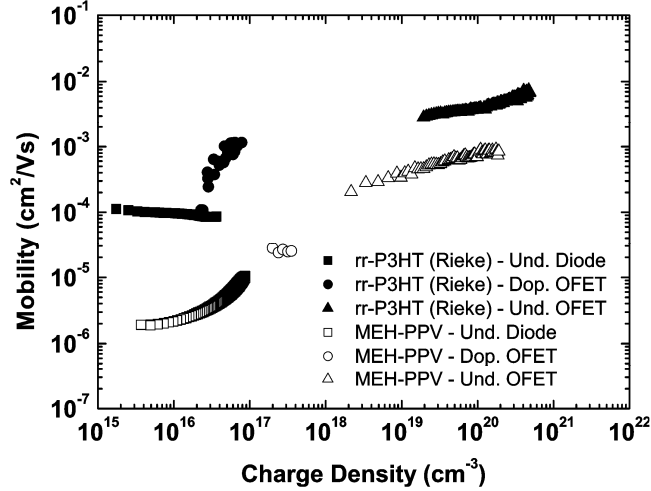


Figure 5. Charge carrier mobility versus carrier density as derived for rr-P3HT (Rieke) and MEH-PPV from undoped (Und.) hole-only diodes, and undoped and doped (Dop.) field-effect transistors.

A second explanation is that differences in conduction might also arise from anisotropy effect due to the nano-crystalline nature of rr-P3HT and other regioregular semiconducting polymers. The anisotropy arises not only from the regioregular or self-organizing nature of polymer materials, but it is also strongly influenced by the solvent, concentration and spincoating conditions [34, 35]. The anisotropy will cause the hopping transport in the material to differ in different directions of conduction. Diodes conduct charges in the perpendicular direction respect to the plane of the spincoated film, while in OFETs there is conduction parallel to the plane. It has already been observed that the packing of rr-P3HT polymer chains is more favorable for the charge transport in the directions parallel rather than perpendicular to the plane of the film, leading to an increased difference in charge carrier mobility between rr-P3HT diodes and OFETs [36]. Hence the stronger the anisotropic effects in a polymer film the stronger the deviation will be from the trend expected from the VMT model. Although anisotropy alone cannot explain the sharp increase in the charge carrier mobility for the doped OFET in Figure 5, it might be the cause of the difference between the hole-only diodes measurements between the two different rr-P3HT batches shown in Figures 4 and 5.

A third possible explanation for the deviation might be the presence of a non-negligible amount of traps in the material. Defects in the polymer chains, chemical impurities and disorder can form trap energy states. If a charge carrier hops unto a

trap state it will become trapped, i.e. immobile, impeding conduction. The release of trapped charge carriers depends on how energetically deep the trap is. The effect of traps is more pronounced at a low carrier density regime as in diodes. In the high charge carrier density regime, as in OFETs, most traps become filled and conduction is not greatly affected. If chemical dopands are introduced into the semiconducting polymer, the extra charge carriers formed by the doping process will fill the traps present in the material, greatly improving the charge carrier mobility at lower charge carrier densities [37], which might explain the sharp increase of the mobility observed in Figure 5.

6.4 Conclusion

In summary, we have experimentally probed the charge carrier mobility as a function of carrier density for rr-P3HT over a wide density range. The mobility at low 10^{15} - 10^{16} cm^{-3} and high 10^{18} - 10^{20} cm^{-3} carrier density was extracted from undoped hole-only diodes and field-effect transistors, respectively. The mobility at intermediate density has been probed by chemically doped Schottky diodes and transistors. We demonstrate that the room temperature mobility is nearly constant at densities below 10^{16} cm^{-3} , whereas the mobility follows a power law for densities higher than 10^{18} cm^{-3} . The mobility at intermediate densities has been probed by chemically doped Schottky diodes and transistors and unites the low- and high density regimes. We also observe that in some materials there can be a deviation from the power law, which can originate either from morphology differences between materials or in the spincoated film, anisotropy effect or significant presence of traps in the material.

References

-
- ¹ R. Coehoorn, W. F. Pasveer, P. A. Bobbert and M. A. J. Michels, *Phys. Rev. B* **72**, 155206 (2005).
 - ² N. Tessler, Y. Preezant, N. Rappaport, and Y. Roichman, *Adv. Mater.* **21**, 2741 (2009).

- ³ V. Coropceanu, J. Cornil, D. a da Silva Filho, Y. Olivier, R. Silbey, and J.-L. Brédas, *Chem. Rev.* **107**, 926 (2007).
- ⁴ I. Fishchuk, V. Arkhipov, A. Kadashchuk, P. Heremans, and H. Bässler, *Phys. Rev. B* **76**, 045210 (2007).
- ⁵ J. Cottaar and P. Bobbert, *Phys. Rev. B* **74**, 115204 (2006).
- ⁶ W. Pasveer, J. Cottaar, C. Tanase, R. Coehoorn, P. Bobbert, P. W. M. Blom, D. M. de Leeuw, and M. Michels, *Phys. Rev. Lett.* **94**, 206601 (2005).
- ⁷ F. Torricelli and L. Colalongo, *IEEE Electron Device Lett.* **30**, 1048 (2009).
- ⁸ C. Tanase, E. J. Meijer, P. W. M. Blom, and D. M. de Leeuw, *Phys. Rev. Lett.* **91**, 216601 (2003).
- ⁹ N. I. Craciun, J. J. Brondijk, and P. W. M. Blom, *Phys. Rev. B* **77**, 035206 (2008).
- ¹⁰ S. P. Speakman, G. G. Rozenberg, K. J. Clay, W. I. Milne, A. Ille, I. A. Gardner, E. Bresler and J. H. G. Steinke, *Org. Electron.* **2**, 65 (2001).
- ¹¹ W. Guangming, J. Swensen, D. Moses and A. J. Heeger, *J. Appl. Phys.* **93**, 6137 (2003).
- ¹² V. D. Mihailetschi, L. J. A. Koster, J. C. Hummelen and P. W. M. Blom, *Phys. Rev. Lett.* **93**, 216601 (2004).
- ¹³ L. Torsi, A. Tafuri, N. Cioffi, M. C. Gallazzi, A. Sassella, L. Sabbatini, and P. G. Zambonin, *Sens. Actuators B* **93**, 257 (2003).
- ¹⁴ M. F. Abasıyanık and M. Şenel, *J. Electroanal. Chem.* **639**, 21 (2010).
- ¹⁵ C. K. Chiang, C. Fincher, Y. W. Park, A. J. Heeger, H. Shirakawa, E. Louis, S. Gau, and A. MacDiarmid, *Phys. Rev. Lett.* **39**, 1098 (1977).
- ¹⁶ A. R. Brown, D. M. de Leeuw, E. E. Havinga, and A. Pomp, *Synth. Met.* **68**, 65 (1994).
- ¹⁷ A. Werner, F. Li, K. Harada, M. Pfeiffer, T. Fritz, K. Leo, and S. Machill, *Adv. Funct. Mater.* **14**, 255 (2004).
- ¹⁸ K.-H. Yim, G. L. Whiting, C. E. Murphy, J. J. M. Halls, J. H. Burroughes, R. H. Friend, and J.-S. Kim, *Adv. Mater.* **20**, 3319 (2008).
- ¹⁹ Y. Zhang, B. de Boer, and P. W. M. Blom, *Adv. Funct. Mater.* **19**, 1901 (2009).
- ²⁰ C. Y. Kao, B. Lee, L. S. Wielunski, M. Heeney, I. McCulloch, E. Garfunkel, L. C. Feldman, and V. Podzorov, *Adv. Funct. Mater.* **19**, 1906 (2009).
- ²¹ M. C. J. M. Vissenberg and M. Matters, *Phys. Rev. B* **57**, 12964 (1998).

-
- ²² F. Maddalena, E. J. Meijer, K. Asadi, D. M. de Leeuw and P. W. M. Blom, *Appl. Phys. Lett.* **97**, 043302 (2010).
- ²³ L. Groenendaal, G. Zotti, P. H. Aubert, S. M. Waybright and J. R. Reynolds, *Adv. Mat.* **15**, 855 (2003).
- ²⁴ L. J. A. Koster, E. C. P. Smits, V. D. Mihailetschi, and P. W. M. Blom, *Phys. Rev. B* **72**, 085205 (2005).
- ²⁵ V. D. Mihailetschi, H. X. Xie, B. De Boer., L. J. A. Koster, and P. W. M. Blom, *Adv. Funct. Mater.* **16**, 699 (2006).
- ²⁶ P. W. M. Blom, M. J. M. de Jong, and M. G. van Munster, *Phys. Rev. B* **55**, R656 (1997).
- ²⁷ G. Horowitz, R. Hajlaoui and P. Delannoy, *J. De Physique III* **5**, 355-371 (1995).
- ²⁸ S. M. Sze and K. K. Ng, *Physics of Semiconductor Devices, 3rd Edition* (Wiley-Interscience, 2006).
- ²⁹ E. J. Meijer, C. Tanase, P. W. M. Blom, E. Van Veenendaal, B.-H. Huisman, D. M. de Leeuw, and T. M. Klapwijk, *Appl. Phys. Lett.* **80**, 3838 (2002).
- ³⁰ E. J. Meijer, C. Detcheverry, P. J. Baesjou, E. van Veenendaal, D. M. de Leeuw and T. M. Klapwijk, *J. Appl. Phys.* **93**, 4831(2003).
- ³¹ R. J. Kline, M. D. McGehee, E. N. Kadnikova, J. Liu and J. M. J. Fréchet, *Adv. Mater.* **15**, 1519 (2003).
- ³² M. Jaiswal and R. Menon, *Polym. Int.* **55**, 1371 (2006).
- ³³ V. I. Arkhipov, P. Heremans, E. V. Emelianova, G. J. Adriaenssens and H. Bässler, *Appl. Phys. Lett.* **82**, 3245 (2003).
- ³⁴ C. Y. Yang, F. Hide, M. A. Díaz-García, A. J. Heeger and Y. Cao, *Polymer* **39**, 2299 (1998).
- ³⁵ T. Nguyen, V. Doan and B. J. Schwartz, *J. Chem. Phys.* **110**, 4068 (1999).
- ³⁶ H. Sirringhaus, P. J. Brown, R. H. Friend, M. M. Nielsen, K. Beckgaard, B. M. W. Langeveld-Voss, A. J. H. Spiering, R. A. J. Janssen, E. W. Meijer, P. Herwig and D. M. de Leeuw, *Nature* **401**, 685 (1999).
- ³⁷ K. F. Seidel and M. Koehler, *Phys. Rev. B* **78**, 235308 (2008).